Numerical and experimental investigation of flow patterns in scraped surface heat exchangers
Proceedings of European Congress of Chemical Engineering (ECCE-6)
Copenhagen, 16-20 September 2007

Numerical and experimental investigation of flow patterns in scraped surface heat exchangers

M. Yataghene[a], F. Fayolle[a], J. Legrand[b]

GEPEA –UMR CNRS 6144
[a]ENITIAA, Rue de la géraudière, BP 82225, 44322 NANTES cedex 3, FRANCE
[b]Université de Nantes, CRTT, BP 406, 44602 SAINT NAZAIRE Cedex, France

Abstract

A numerical investigation of a scraped surface heat exchanger was undertaken using the commercial CFD code FLUENT in order to characterize the flow patterns for Newtonian and Non-Newtonian highly viscous fluids where experimental measurements are difficult to obtain. Simulation results were validated with experimental shear rates measured using electrochemical method (Mabit et al., 2003) as well as velocity profiles obtained by PIV. Two different flow configurations were treated separately: first, the inlet bowl not reached by the scraping blades, and second the exchanger itself, with two scraping blades. In the inlet bowl, velocity profiles calculated show a dead zone where clogging can occur. In the exchange part itself, the zone localized between the tip of the blades and the stator has to be studied more carefully. Laminar isothermal steady-state flow was studied in a 2D cross section of the exchanger. Comparison between predictions and experimental measurements gave good agreement.

Keywords: surface scraped heat exchanger, CFD, PIV, viscous fluids, laminar flow

1. Introduction

In the food and chemical industries, scraped surface heat exchangers (SSHE) are widely used for heating or cooling of viscous fluids. Blades mounted on a rotating shaft continuously remove the product in contact with the exchange surface, inducing radial mixing and improving heat transfer. In this type of apparatus, the flow is the result of the superposition of an annular Poiseuille flow and a Taylor-Couette flow, on which perturbations are added by blade rotation. Experimental and numerical studies have been realised and the presence of vortices has been identified, in particular Taylor vortices which were visualised by Naimi (1989) and Dumont et al. (2000a, b) for Ta_g values from 61 to 80 depending on product properties. Taylor vortices appear

at the outlet and move throughout the exchanger towards the inlet bowl. Dumont et al. (2002) have shown, using an electrochemical method, the presence of high wall shear rates at the scraped exchange surface. Blade scraping caused high perturbations at the surface and a large increase of shear stress was observed. Numerical studies (De Goede and De Jong, 1993, Stranzinger et al., 2001) reveal the appearance of heterogeneities for specific conditions of Taylor number leading to heterogeneous thermal treatment. Mabit et al. (2003) have also shown that Taylor vortices can reach the inlet and outlet bowls from high rotation velocities.

Whereas the presence of Taylor vortices enhances mixing and thus tends to decrease thermal heterogeneities, in most cases, complex products have to be treated at low rotating velocity in order to avoid change of their texture. In this case, good thermal treatment may not be ensured any more, and renewal of the product at the exchange surface thanks to the blade is also reduced. Meanwhile, with highly viscous fluids, there is a high probability for the fluid to clog at the surface of the inlet bowl, not reached by the scraping blades.

Because of the complex geometry of SSHEs, experimental measurements are difficult to handle. Most of the time, it is necessary to separate hydrodynamics studies (Trommelen and Beek, 1971, De Goede and De Jong, 1993) from thermal studies (Lakhdar et al.,2005, Maingonnat and Corrieu, 1983). Hydrodynamic measurements most of the time need transparent body of the apparatus (PIV for example), and need to be conducted in isothermal conditions. Moreover, some particular part of the system may not be reachable by the measuring techniques. Bowls, with their particular geometry, are in this case. One of the interests of CFD modeling is to give information where no experimental investigations can be handled. When hydrodynamics is well understood, it is then possible to help industrials choose the optimal operating conditions for their process. The second interest is that it is possible with CFD to couple hydrodynamics with thermal calculations.

The aim of this work is to realise CFD simulation of both parts of the exchanger:
-   first the inlet bowl in order to identify dead zones where clogging can occur,
-   second in the exchanger part itself.

Before using the model in thermal treatment, this paper presents results obtained with isothermal simulations validated against experimental results.

The evolution of the flow pattern is analysed for Newtonian and non-Newtonian highly viscous products.

2. Materials and methods:

2.1. Experimental set up

The work was carried out on a scaled-down model of an industrial exchanger: Duprat TR 13x60 (Figure 1). All dimensions are given in previous work (Mabit et al., 2003). This scaled-down model was built in order to present the same thermal behaviour as the one obtained in the industrial SSHE. It was equipped with electrochemical probe to measure shear stress and to understand hydrodynamic behaviour. Measurement of local shear rates in the inlet bowl were handled by Mabit et al. (2003) using electrochemical method will not be described here.
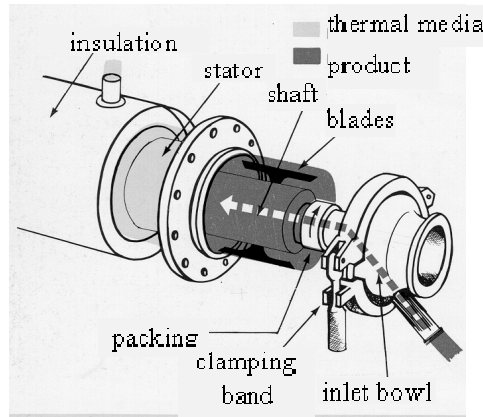
Figure 1: Scheme of the SSHE (by courtesy of Duprat SA)

2.2. PIV measurements

Particle Image Velocimety (PIV) has been used in order to determine velocity profiles in laminar flow, in the exchanger as well as the inlet bowl. The same scaled-down exchanger as for electrochemical measurement was used. However, the "bowl shaped" inlet corresponding to industrial exchangers had to be straightened in order to prevent laser diffraction through the transparent wall.

The system is composed of 1 camera (Canon Mega-Plus, resolution 1600*1186 pixels), a pulsed laser Nd-YAG (wavelength λ=532nm, pulse energy =15mJ), and a processor equipped with "Flowmanager" software (from DANTEC). The experimental technique used is the same as the one described by Aloui *et al.* (2006). Velocity profiles are recorded both in the x,y plane and in the y,z plane (Figure 2). Dotted lines represent the position of the cross section where velocity profiles were measured, respectively: (a) cross section in the inlet bowl, (b) in the exchanger before the edge of the blade, (c) in the passage of the blade, before its fixation point, and (d) after the fixation point.
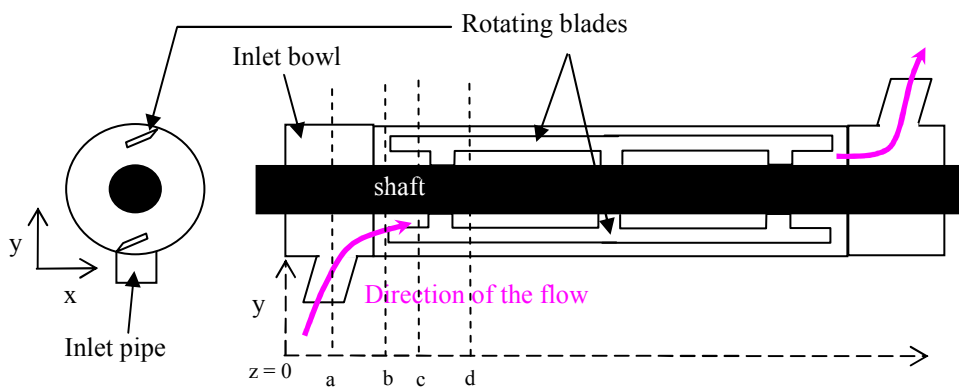
Figure 2: Scheme of the ESR and position of the PIV measurements
a = 49 mm, b = 83 mm, c = 93 mm, d = 113 mm

Spherical seed particles of Polyamide (PSP, 50 µm mean diameter, 1030 kg/m^3) were dispersed in the working fluids, their density being of the same order of magnitude as

the working fluids in order to prevent sedimentation. Because of the rotation of the blade, a synchronisation of the acquisition is necessary in order to obtain the same position of the blade in all images captured by the camera. Then, when permanent regime is reached in laminar flow, the average statistical velocity vector on each point is calculated from100 images pairs. The image data were analysed with a multi-pass adaptation cross correlation technique with 64x64 pixels interrogation windows and overlap of 50% on the final pass. The standard deviation was verified and was very small. The rotor is in stainless steel, and not transparent to the laser beam, therefore, the velocity profiles can not be measured directly in the hidden part of the bowl. In the exchange part, a mirror was used in order to reflect the laser beam and to reach the whole cross section.

An image of the seeded fluid recorded in the bowl is presented on figure 3 as an example.
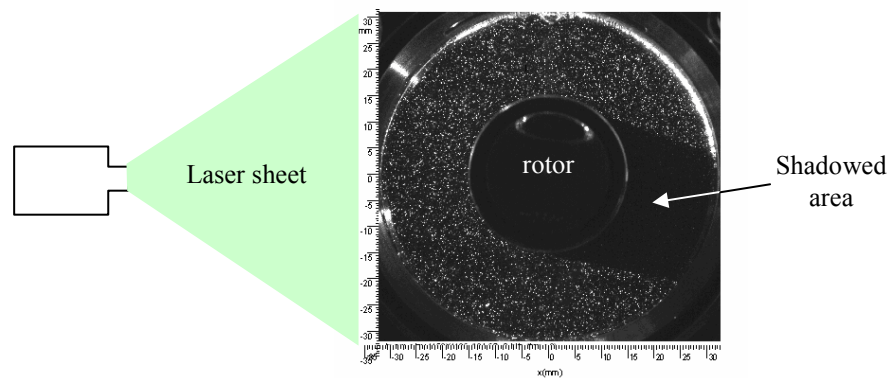
Figure 3: Image taken by the camera placed perpendicularly to the laser sheet

2.3. Working fluids

Three types of fluids were used: Newtonian pure glycerol and HV45 (with 25% water) and shear thinning CMC (1% w/w in water). All physical properties are given in table 1.

	Glycerol	HV45	CMC 1%
Viscosity (at 20°C)	1.2 Pa.s	0.84 Pa.s	*Cross model* $$\eta_{app} = \frac{14.88}{1 + 0.93\dot{\gamma}^{0.69}}$$
density	1240 kg/m^3	1079 kg/m^3	1047 kg/m^3

2.4. CFD calculations

Because of the presence of the blades, and especially because of the small gap present between the tip of the blades and the exchange surface, a 3D simulation of the whole exchanger is very difficult, especially for creating the mesh necessary for the simulation. Therefore, the exchanger was separated in 2 different regions:
-   the inlet bowl, not reached by the blades, where a 3D simulation was conducted
-   the exchanger itself, where 2D simulations of cross sections were performed at the same z position as the PIV measurements.

Fluent software was used to realise the simulation. Scheme of both meshes, created by Gambit, are presented in figure 4.
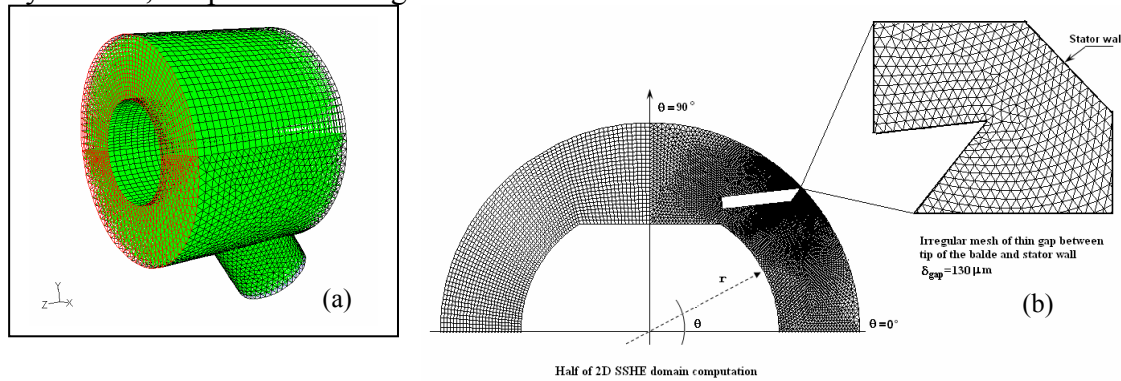
Figure 4: Scheme of the meshes used for the CFD simulation
(a) inlet bowl, (b) cross section of the scraped domain

Details on the 2D simulation are given by Yataghene *et al* (2007): boundary conditions, grid independency… and will not be discussed further.

In the inlet bowl, two domains are modelled consecutively: the inlet pipe, without any rotating part, and the bowl itself, with the rotating shaft. For the calculation, the rotor is considered as a moving wall, with angular velocity Ω, and the stator is immobile.

Velocity profiles were calculated for glycerol, HV45 and CMC solutions, using the physical properties given in table 1.

All velocity magnitudes are presented in m/s, both for experiments and CFD results.

3. Result and discussion

3.1. Inlet bowl

3.1.1. Comparison of CFD and electrochemical measurements of the shear rates

Simulations were first validated with shear rates measured by Mabit et al. (2003). Figure 5 shows the shear rates measured for HV45 on the bowl surface and on the rotor for rotating velocities from 0.5 to 4 rotations per second (rps). The flow rate was 35 l/h. As seen on figure 5, simulations are in very good agreement with measured shear rates.
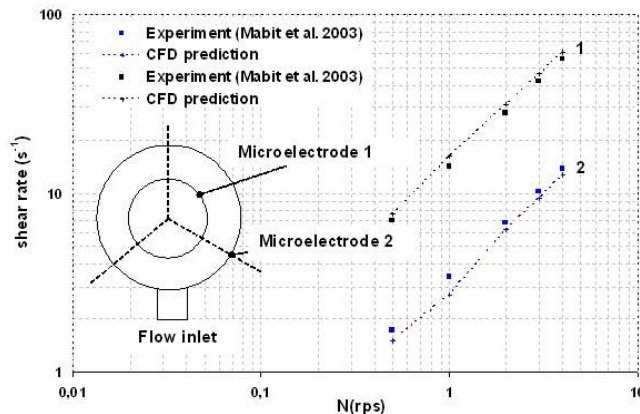
Figure 5: Shear rates in the inlet bowl for HV45

The interest of the simulation is to give velocity profile in the whole domain, whereas measurements can only be done on fewer points. Figure 6 show the result of the velocity magnitudes calculated for HV45 with Q= 150 l/h, and N = 2 rps. Even for such high flow rates, it can be seen that the flow is mainly due to the rotation of the shaft. At the top of the bowl, and at the junction between the bowl and the inlet pipe, the velocity is very low, creating a dead zone, where there is a high probability for the product to stay longer than in the rest of the bowl. In industrial uses, thermal treatment does not begin in the inlet bowl, so, the quality, and time, of the thermal treatment may not be influenced by these heterogeneous residence times in the bowl. However, for such high viscosities, the product will stick at the surface, and a layer of stuck product can be created, leading to a degradation of the product, and decreasing the cleanability of the exchanger.
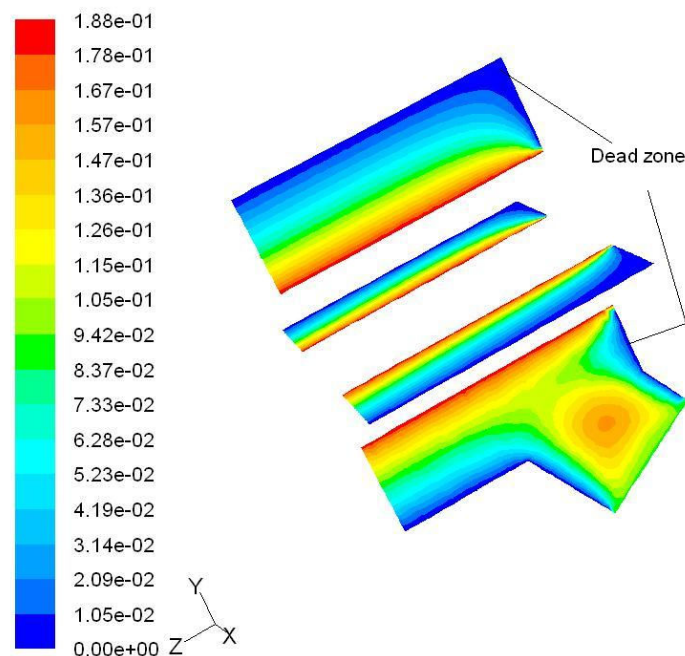
Figure 6: velocity magnitude for HV45 (Q=150 l/h, N = 2 rps)

Nether the less, it has to be noted that the simulated bowl was chosen in order to represent the same geometry as the one used for PIV measurements. As said before, industrial geometries have been improved in order to limit clogging effects and simulations such as the one presented here is an interesting tool for exchanger manufacturers in order to obtain the most appropriate geometry to prevent clogging.

3.1.2. Comparison with PIV measurements

Shear rates represent the velocity gradients, measured on surfaces. Therefore, the results presented formerly only validate the limit conditions of our model. It is now necessary to validate the velocity profile in the whole simulation domain. Figure 7 and 8 show velocity profiles for position (a) in the inlet bowl, for glycerol and CMC respectively, at Q= 150 l/h and N = 3 rps.

Numerical result   PIV Result
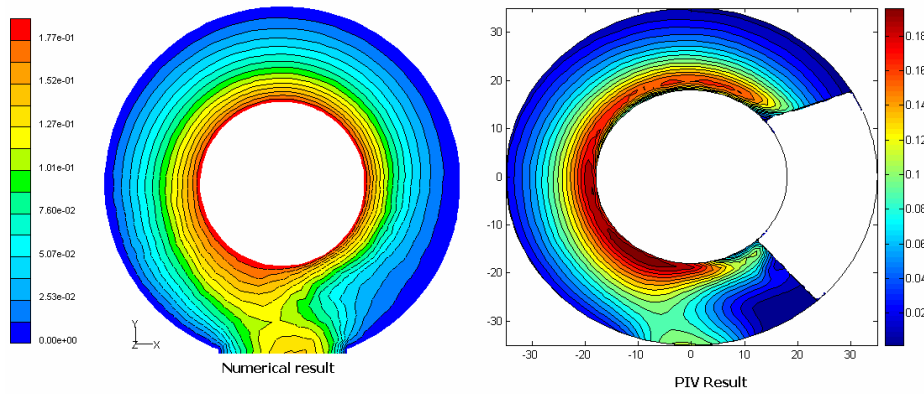
Figure 7: Velocity profiles for glycerol

CFD result   PIV result
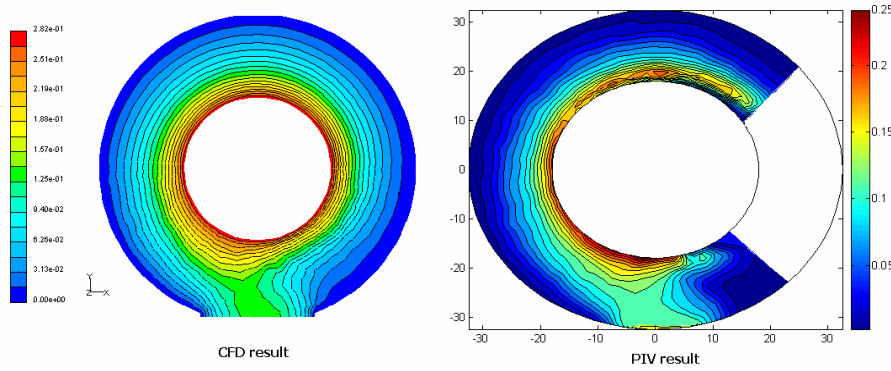
Figure 8: velocity profiles for CMC 1%

Figure 9 represent the velocity profiles at the junction of the inlet pipe and the bowl for CMC. Again, CFD results are in very good agreement with experimental velocity profiles.
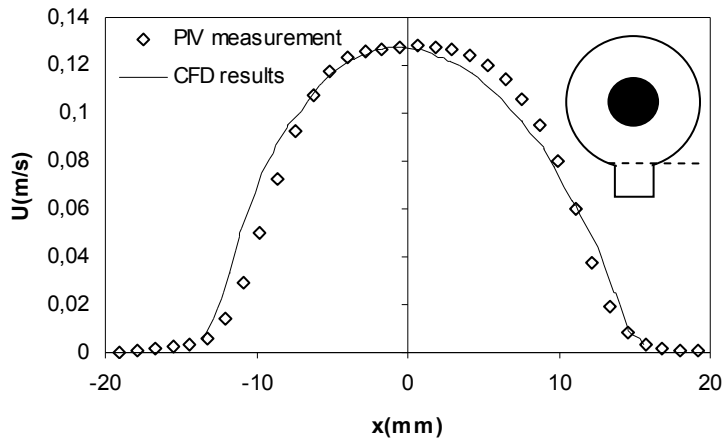
Figure 9: Velocity profile at the junction with the inlet pipe for CMC 1%

3.2. Modeling of the cross section of the exchanger

As explained before, CFD simulation in the exchanger itself is done on a 2D cross section because of the presence of the small gap between the tip of the blade and the exchange surface. Therefore, the validation of the model was first done using PIV

measurements with no axial flow rate. Figure 10 shows results for glycerol at N= 5 rps, on the (c) plane, where the influence of the blade is well identified.

Both experimental and CFD results show that the flow is mainly imposed by the rotation of the blade. Velocity gradients are very important close to the blade, which confirms the very high shear rates identified by Dumont *et al.* (2000a, b).

CFD Result   PIV result
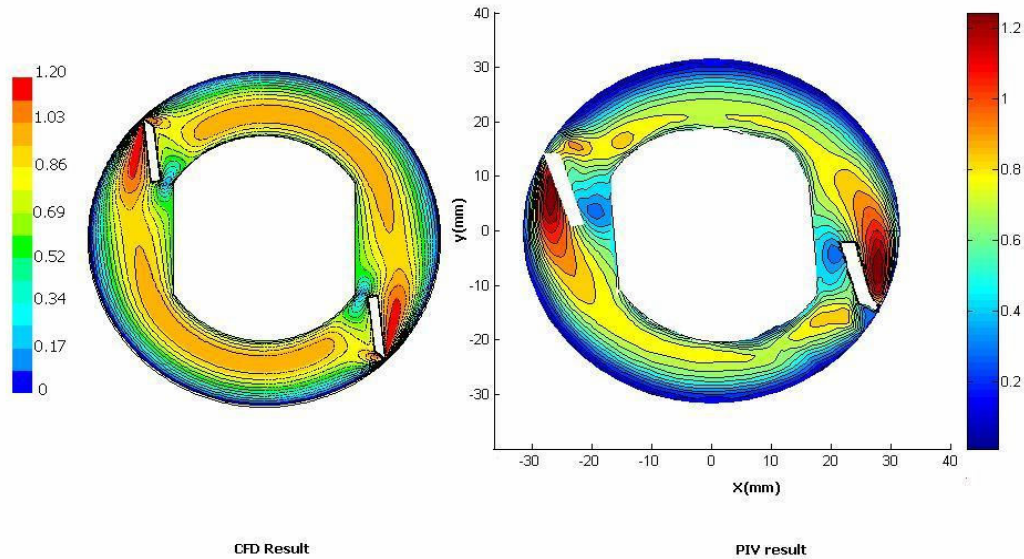
Figure 10: flow pattern in the exchanger for glycerol, (c) position,

Once the validation is completed, the interest of the model is to give more complete information about the local flow pattern in the SSHE. Figure 11 shows the velocity field vectors at the tip of the blade. A recirculation just after the passage of the blade is identified by the calculations, which confirm that the flow behaviour in the type of exchanger is very complex.
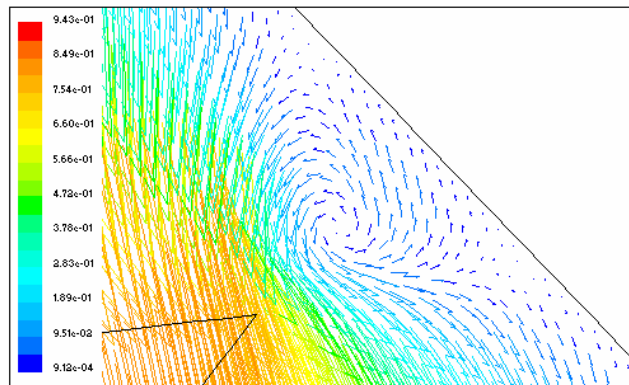
Figure 11: velocity field vectors at the tip of the blade of CMC

Simulation can also give information on apparent viscosity profiles in the exchanger, especially close to the wall. As suspected by Fayolle et al. (2005), because of the high shear rates, viscosity decreases drastically at the surface, which creates two separate flows: one with very low viscosity at the exchange surface, and another one with higher viscosity close to the rotor, with very little mixing between one another.

4. Conclusion

This work presents flow pattern inside a scraped surface heat exchanger obtained both by experimental methods (electrochemistry and PIV) and by CFD calculations. The global aim of our studies was:

- First to verify in a geometry adapted for experimental set-up, that CFD model was able to give reliable results. Two different zones were studied, the inlet bowl, with no blades, and the exchanger itself. All the CFD simulations presented agree very well with experimental results.
- Second, to understand more precisely the flow pattern in the exchanger. In the inlet, dead zones have been identified by the model, which were difficult to see only with experimental results. In the exchanger, the velocity profile at the tip of the blade is also better identified. In both case, the model gives valuable information, complementary to experiments.
- Third, and still to be done, to help exchanger manufacturers in the conception of more appropriate geometries, with no dead zones, as well as exchanger users in the choice of their operating conditions. Now that the aptitude of the model to simulate correctly simple geometries, it will be possible to change the geometry modelled and conceive the best possible one.

References

Aloui F. Rehimi F., Ait Mouheb N., Ben Nasrallah S., Doubliez L., (2006*) Congrès Francophone de Techniques Laser*, Toulouse (France) 19-22 sept 2006
Dumont E., Fayolle F., Legrand J., (2000a) *J. of Food Eng.*, **45**, 4, 195-207
Dumont E., Fayolle F., Legrand J., (2000b) *AIChE Journal*, **46,** 6, 1138-1148,
De Goede R. and De Jong E. J., (1993) *Chem. Eng. Science*, **48,** 1393-1404
Fayolle F., Mabit J., Legrand J.(2005) *J. of Appl. Electrochem.*, **35**, 487-498
Lakhdar M. B., Cerecero R., Alvarez G., Guilpart J., Flick D. and Lallemand. A., (2005) *Applied Thermal Eng.,* **25** 45-60
Maingonnat F. and Corrieu G., (1983) *Entropie,* **111,** 37-48
Mabit, J., Fayolle, F. and Legrand, J., (2003) *Chem. Eng. Science,* **58**, 20, 4667-4679
Naimi M., (1989), *PhD Thesis*, INP Lorraine
Stranzinger M., Feigl K. and Windhab E., (2001) *Chem. Eng. Science*, **56**, 3347-3363.
Trommelen A. M. and Beek W. J., (1971) *Chem. Eng. Science*, **26**, 1933-1942
Yataghene M., Pruvost J., Fayolle F., Legrand J. (2007), *Chem. Eng. and Proc.*, accepted for publication.